ChemComm
Chemical Communications

Accepted Manuscript

This article can be cited before page numbers have been issued, to do this please use: L. Quan, J. Gu, W. Lin, Y. Wei, Y. Lin, L. Liu, H. Ding, C. Pan, Z. Xie and T. Wu, *Chem. Commun.*, 2019, DOI: 10.1039/C9CC03810H.




ROYAL SOCIETY OF CHEMISTRY

rsc.li/chemcomm

View Article Online
DOI: 10.1039/C9CC03810H

COMMUNICATION

# BODIPY Biosensor to Detect and Drive self-assembly of Diphenylalanine

Received 00th January 20xx,
Accepted 00th January 20xx

DOI: 10.1039/x0xx00000x

Li Quan,*[a] Jianhua Gu,[d] Wenhai Lin,[b] Yanchun Wei,[a] Yuebin Lin,[a] Lei Liu,[a] Hongyan Ding,[a] Changjiang Pan,[a] Zhigang Xie,**[b] Tianfu Wu***[c]

**Diphenylalanine (FF), as the smallest unit and core recognition motif of β-amyloid (Aβ), could self-assemble into nanofibers, which induces early onset of Alzheimer's disease (AD). Green/near-infrared fluorescencent BODIPY probes were designed and synthesized to detect FF-assembly, providing unique insights into the chemical and molecular mechanism of Aβ aggregation and drug development for AD.**

AD is an incurable condition. To date, none of the clinically tested drugs have shown significant effectiveness.[1–4] Therefore, it is urgent to seek effective therapeutics and imaging probes capable of assisting the drug development. It is proverbial that the aggregation of β-amyloid (Aβ) plays a central role in the neuropathology of AD.[5–7] In the past decades, researchers have been exploring AD associated molecular basis and aggregation mechanisms, which include hydrogen bonding, hydrophobic interactions, and steric interactions.[3, 7–17] The interactions between aromatic moieties often play a key role in facilitating molecular recognition which further leads to enhanced protein/peptide aggregation.[10,17] The aggregation pattern has prompted the search for the mechanisms of disease progression and novel treatment options for AD. To our interest, the familial mutations of Aβ within the polypeptide translated region leading to the early onset of AD, such as Iowa, Arctic, Dutch, Italian, Ottawa and Flemish mutations, are located adjacent to FF region.[18] Therefore, we believe that diphenylalanine (FF) plays a significant role in the initial steps of Aβ interaction which leads to the formation of plaques. FF as a hydrophobic residue at the C-terminus of Aβ was identified as the smallest unit or the core recognition motif of Aβ polypeptide.[19-21] FF could self-assemble into ordered structures with a green-gold birefringence upon staining with Congo red dye, which is similar to the amyloid structures, indicating that FF contains all the molecular information needed to mediate self-assembly into regular structures.[10] The similar photoluminescence properties of labelled FF modules,[22] aggregation patterns of polypeptides[23,24] as well as their mechanical properties,[25–27] are indicative of a common generic form of noncovalent packing of Aβ. FF region thus represents both a key molecular recognition and self-assembly unit as shown in **Scheme 1**, as well as a potential drug target for efficient inhibition of the amyloidogenic process. Therefore, the development of novel probes to detect FF-assembly may open up a new avenue towards early diagnosis (via imaging) of AD.

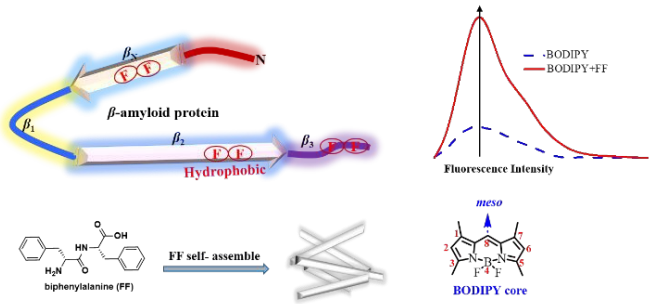


**Scheme 1**. FF, the smallest unit of β-amyloid (Aβ) protein, could be detected via specific binding by a novel fluorescent probe of a BODIPY derivative.

In recent decades, an emerging fluorescent dye, BODIPY (boron-dipyrromethenes, **Scheme 1**), has gained extensive attention in the field of biomedical and molecular probes due to its excellent optical stability, high fluorescence quantum yield, molar extinction coefficient, easy modification and so on.[28] Synthesis of BODIPY with different excitation and emission wavelengths by introducing different substituents to the peripheral location of BODIPY core has attracted extensive attention.[29,30] The following methods are often adopted: (1) conjugation of responsive rings; (2) introduction of double bonds and other structures in 3 and 5 positions to extend the matron conjugate; (3) conjugation of 2, 3 and 5, 6 aromatic rings; (4) conjugation of 1, 7, 8 bit aromatic rings; (5) replacement of C atoms with N atoms in *meso*, 2, 6 position. In this paper, BODIPY probes to achieve fluorescence wavelength

[a] *Department of Mechanical and Material Engineering, Huaiyin Institute of Technology, Huai'an 223003, Jiangsu Province, China.*
[b] *State Key Laboratory of Polymer Physics and Chemistry, Changchun Institute of Applied Chemistry, Chinese Academy of Sciences, Changchun 130022, China.*
[c] *Department of Biomedical Engineering, University of Houston, Houston, Texas 77204, USA.*
[d] *Electron Microscopy Core, Houston Methodist Research Institute, Houston, TX 77030, USA.*
† Footnotes relating to the title and/or authors should appear here.
Electronic Supplementary Information (ESI) available: [details of any supplementary information available should be included here]. See DOI: 10.1039/x0xx00000x

ranging from 400nm to 800nm were designed and synthesized. Starting from the commercially available pyrrole-based starting materials, it is relatively easy to produce a multitude of BODIPY dyes, often in high yield and multi-gram quantity. Interestingly, spectroscopic/ photophysical properties could be "fine-tuned" by introducing different electron releasing/ withdrawing groups onto the BODIPY framework.[31,32] Response of BODIPY to FF was identified by electron microscope (SEM), fluorescence spectrophotometer (FL) and confocal microscopic imaging (CMI).

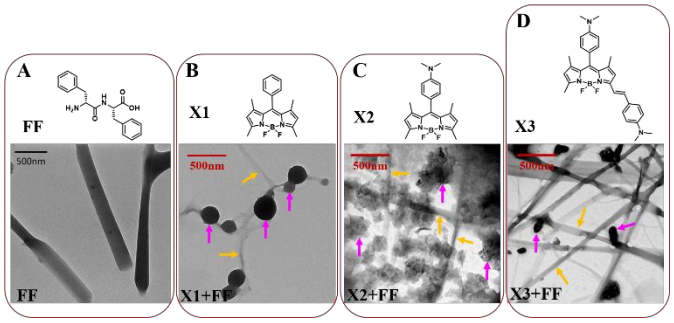


**Figure 1**. SEM of self-assembly of FF and response of BODIPY probes to FF. A) FF nanofibers; B) X1 and FF nanofibers; C) X2 and FF nanofibers; D) X3 and FF nanofibers. The magenta arrow identifies BODIPY and the orange arrow identifies FF nanofibers.

Firstly, the three BODIPY molecules (X1, X2 and X3) were analyzed for their responses to FF nanofibers based on FL (**Figure S1**, **S2**). In order to quantify their responses to FF nanofibers, each probe and FF nanofibers were used at the same concentrations and amount. X2 showed poor responses to FF nanofibers (**Figure S1**, **S2**). X3 showed significant responses to FF nanofibers with 150% increased fluorescence intensity when attached to FF nanofibers, but the total fluorescence intensity was very low (12 a.u., with 1ml X3 at 0.05mM and 10 µl FF nanofibers at 0.22mg/ml), hence not suitable as a fluorescent probe. In comparison, when X1 was bound to FF nanofibers, the fluorescence intensity was increased by 360% ($\Delta F/F$) with very high fluorescence intensity (904 a.u., with 1ml X1 at 0.05mM and 10µl FF nanofibers at 0.22mg/ml) (**Figure S2**). Although the $-NH_2$ group in *meso*-phenyl of X3 improved the recognition performance of the probe, it exhibited a significant negative impact on the fluorescence intensity of the BODIPY probes because photo-induced electron transfer (PET) led to decreased fluorescence. Moreover, BODIPY is a conjugated compound, and *meso*-phenyl of BODIPY can rotate within a certain spatial range. When BODIPY probe responds to FF, the *meso*-phenyl is well planar with the conjugate system of BODIPY (**Figure S3**) leading to enhanced fluorescence. For free X1, the *meso*-phenyl could rotate freely, and the conjugated system had an emission peak at 523 nm. When X1 was bound to FF nanofibers, X1's emission peak shifted to 526 nm, and the *meso*-phenyl kept well planar to the whole BODIPY conjugated system. (**Table S1**). This red shift suggests an effective π-π stacking between the aromatic residues, possibly in a J-aggregate fashion.[33]

SEM analysis further verified the responses of X1 to FF nanofibers. As shown in **Figure 1**, FF was self-assembled into nanofibers (**Figure 1A**). X1 and X3 were distributed and adhered only to FF nanofibers (**Figure 1B**, **1D**). In comparison with random attachment of X2 to FF nanofibers (**Figure 1C**). This experiment indicates that X1 and X3 were selectively attached to FF nanofibers. However, the fluorescence of X3 was too weak to be used as an effective fluorescent detector (**Figure S1** and **S2**). With the consistent results from fluorescence imaging and SEM analysis of X1, X2 and X3, we concluded that X1 was the most robust responder to FF nanofibers.

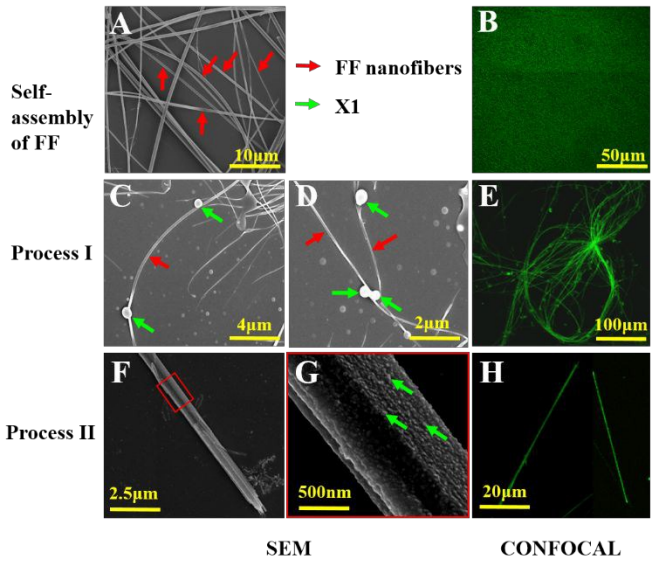


**Figure 2**. FF self-assembly process demonstrated by SEM and laser confocal fluorescence imaging. There are two distinct assembly processes: in Process I, FF was self-assembled alone to form nanofibers (C, D, E); whereas in Process II, FF was assembled together with BODIPY probe X1 to form nanofibers (F, G, H). A) SEM of self-assembly of FF without staining; B) laser confocal fluorescence imaging of self-assembly of X1; X1 was added onto self-assembled FF on silicon wafer (C, D); co-assembly of FF-X1 using the mixture solution of FF and X1 on silicon wafer (F, G); confocal fluorescence imaging of (C, D) is shown in E and the confocal imaging of (F, G) is shown in H. C and D show different areas on the silicon wafer. G is the zoomed-in image of the red-rectangle area in F. The red arrows point to FF nanofibers, and the green arrows point to X1 assembly.

As the smallest unit of Aβ, FF could assemble into nano-frameworks and even simulate Aβ aggregation. We are interested to uncover the mechanism by which FF is assembled. Here we designed two assembly processes and investigated them by SEM and CMI. As far as we know, the self-assembly morphology usually depends on the molecular and solution parameters. For a given molecule, although its molecular parameters such as hydrophobic or hydrophilic properties and the architecture are constant, a different morphology can still be obtained by tuning solution parameters such as the type of solvents, solvent quality, the molecule concentration, the pH value and temperature, etc.[34] In this paper, when the FF monomers was first dissolved in 1,1,1,3,3,3-hexafluoro-2-propanol (HFP) and then added into water, they were rapidly self-assembled into nanofibers. These FF nanofibers exhibited certain structural flexibility (**Figure 2A**). However, when X1

solution was added into FF nanofibers (in water), X1 was self-assembled into nanospheres and simultaneously bound to FF nanofibers selectively (**Figure 2C**, **2D**). In order to verify that X1 was indeed self-assembled into nanospheres in water, X1's HFP solution was added into water. As a result, the self-assembled morphology of nanospheres was shown in SEM results (**Figure 2B**). In this process (Process I), X1 didn't change the properties of FF nanofibers and was only tightly adhered to FF nanofibers to make a clear fluorescent imaging of the flexible FF nanofibers (**Figure 2E**). In another assembly process (Process II), the co-assembly was investigated. To our surprise, FF and X1 were able to co-assemble in water. In this co-assembly process, X1 drove FF to assemble into fluorescent nanofibers with higher rigidity (**Figure 2F**, **2G**). Because X1 and FF molecules were orderly bound to each other to avoid aggregation-induced fluorescence quenching, a clear fluorescent image of rigid straight nanofibers were demonstrated by CMI (**Figure 2H**). In contrast, X2 or X3 couldn't drive FF to co-assemble into nanofibers (**Figure S4**).

Furthermore, the specificity of X1 in binding to FF nanofibers was verified by Atomic Force Microscope (AFM) (**Figure S5**). AFM has been considered as a powerful tool in analyzing the interaction forces between two molecules.[35-37] Here we used AFM to measure the interaction forces between X1 and FF nanofibers and to determine the specific binding of X1 to FF nanofibers. Our results clearly exhibited a significant interaction force of 0.53nN between X1 and FF nanofibers (**Figure S5a**), which is much higher than that between X1 and Trpytophan (0.075nN) (**Figure S5b**). In addition, the test substrate, mica, had little-to-no interaction with BODIPY (0.002nN) (**Figure S5c**). Strong adhesion forces between X1 and FF nanofibers occurred very frequently as shown in **Figure S5a**. This additional experimental data strongly supported the specificity of our X1 biosensor in detecting FF nanofibers.

## Conclusions

It is known that the familial mutations within the Aβ polypeptide translated region leading to the early onset of AD, are located adjacent to FF region. Three BODIPY probes were designed and synthesized to detect FF. We found the structures of the probes play a key role in response to FF assembly, and planar conjugation is the most important factor. In the screening of fluorescence probes in this paper, high fluorescence efficiency was used as the primary criteria for success. We have demonstrated that the BODIPY probe X1 exhibited specific responses to FF nanofibers with strong fluorescence. When binding to FF, X1's fluorescence intensity was increased by 360% folds (ΔF/F). This probe may be potentially useful in the early diagnosis (via imaging) of AD.

## Acknowledgement

This work was supported by grants from the start-up fund of Huaiyin Institute of Technology, the Natural Science Foundation of Jiangsu Provincial Department of Education (17KJB530001), the Natural Science Foundation of China (51803068 and 31470926), Jiangsu Government Overseas Studies Scholarship (JS-2017-201), the International Cooperation in Science and Technology Research projects (HAC201615), and Jiangsu Qing Lan project.

## Notes and references

**Corresponding Author**
* Li Quan; E-mail: quanxiaofei2018@gmail.com.
**Zhigang Xie; E-mail: xiez@ciac.ac.cn.
***Tianfu Wu; E-mail: twu13@central.uh.edu.

1 T. P. J. Knowles, M. Vendruscolo, C. M. Dobson, *Nat. Rev. Mol. Cell Biol.,* 2014, **15**, 384.
2 D. Eisenberg, M. Jucker, *Cell,* 2012, **148**, 1188.
3 A. Aguzzi, T. O'Connor, *Nat. Rev. Drug Discovery,* 2010, **9**, 237.
4 E. A. Gazit, *FASEB J.,* 2002, **16**, 77.
5 A. F. McKoy, J. Chen, T. Schupbach, M. H. Hecht, *J. Biol. Chem.,* 2012, **287**, 38992.
6 O. S. Makin, L. C. Serpell, *FEBS J.*, 2005, **272**, 5950.
7 W. Kim, Y. Kim, J. Min, D. J. Kim, Y. T. Chang, M. H. Hecht, *ACS Chem. Biol.,* 2006, **1**, 461.
8 B. E. Roberts, J. Shorter, *Nat. Struct. Mol. Biol.* 2008, **15**, 544.
9 K. Ono, Y. Yoshiike, A. Takashima, K. Hasegawa, H. Naiki, M. Yamada, *J. Neurochem*., 2003, **87**, 172.
10 A. P. Pawar, K. F. DuBay, J. Zurdo, F. Chiti, M. Vendruscolo, C. M. Dobson, *J. Mol. Biol.,* 2005, **350**, 379.
11 A. Aguzzi, A. M. Calella, *Physiol. Rev.* 2009, **89**, 1105.
12 A. Kapurniotu, *Chem. Bio. Chem.,* 2012, **13**, 27.
13 M. Jin, N. Shepardson, T. Yang, G. Chen, D. Walsh, D. J. Selkoe, *Proc. Natl. Acad. Sci. U. S. A.,* 2011, **108**, 5819.
14 G. M. Shankar, S. Li, T. H. Mehta, A. Garcia-Munoz, N. E. Shepardson, I. Smith, F. M. Brett, M. A. Farrell, M. J. Rowan, C. A. Lemere, C. M. Regan, D. M. Walsh, B. L. Sabatini, D. Selkoe, *J. Nat. Med.,* 2008, **14**, 837.
15 A. Lakshmanan, D. W. Cheong, A. Accardo, E. D. Fabrizio, C. A. E. Hauser, *Proc. Natl. Acad. Sci. U. S. A.,* 2013, **110**, 519.
16 F. T. Senguen, T. M. Doran, N. R. Lee, E. A. Anderson, X. Gu, D. M. Ryan, B. L. Nilsson, *Mol. BioSyst.,* 2011, **7**, 486.
17 R. Cukalevski, B. Boland, B. Frohm, E. Thulin, D. Walsh, S. Linse, *ACS Chem. Neurosci.,* 2012, **3**, 1008.
18 T. J. Grabowski, H. S. Cho, J. P. G. Vonsattel, *Ann. Neurol.,* 2001, **49**, 697.
19 M. Reches, E. Gazit, *Science,* 2003, **300**, 625.
20 M. Reches, E. Gazit, *Isr. J. Chem.,* 2005, **45**, 363.
21 W. Kim, M. H. Hecht, *Natl. Acad. Sci. U. S. A.,* 2006, **103**, 15824.
22 N. Amdursky, M. Molotskii, D. Aronov, L. Adler-Abramovich, E. Gazit, G. Rosenman, *Nano Lett.,* 2009, **9**, 3111.
23 D. Pinotsi, A. K. Buell, C. M. Dobson, G. S. Kaminski Schierle, C. F. Kaminski, *Chem. Bio. Chem.,* 2013, **14**, 846.
24 E. K. Esbjörner, F. Chan, E. Rees, M. Erdelyi, L. M. Luheshi, C. W. Bertoncini, C. F. Kaminski, C. M. Dobson, G. S. Kaminski Schierle, *Chem. Biol.,* 2014, **21**, 732.
25 T. P. J. Knowles, M. J. Buehler, *Nat. Nanotechnol.,* 2011, **6**, 469.
26 N. Kol, L. Adler-Abramovich, D. Barlam, R. Z. Shneck, E. Gazit, I. Rousso, *Nano Lett.,* 2005, **5**, 1343.
27 I. Azuri, L. Adler-Abramovich, E. Gazit, O. Hod, L. Kronik, *J. Am. Chem. Soc.,* 2014, **136**, 963.
28 Z. Guo, Y. Zou, H. He, J. Rao, S. Ji, X. Cui, H. Ke, Y. Deng, Yang, H.; Chen, C.; Zhao, Y.; Chen, H. *Adv. Mater.,* 2016, **28**, 10155.
29 H. Lu, J. Mack, Y. Yang, Z. Shen, *Chem. Soc. Rev.,* 2014, **43**, 4778.
30 L. Y. Niu, Y. S. Guan, Y. Z. Chen, L. Z. Wu, C. H. Tung, Q. Yang, Z. *J. Am. Chem. Soc.,* 2012, **134**, 18928.

View Article Online
DOI: 10.1039/C9CC03810H

31 L. Quan, S. Liu, T. T. Sun, X. G. Guan, W. H. Lin, Z. G. Xie, Y. B. Huang, Y. Q. Wang, X. B. Jing, *ACS Appl. Mater. Interfaces,* 2014, **6**, 16166.
32 N. Boens, V. Leen, W. Dehaen, *Chem. Soc. Rev.,* 2012, **41**, 1130.
33 X. H. Yan, P. L. Zhu, J. B. Li, *Chem. Soc. Rev.,* 2010, **39**, 1877.
34 P. Bhargava, Y. F. Tu, J. X. Zheng, H. M. Xiong, R. P. Quirk, S. Z. D. Cheng, *J. Am. Chem. Soc.,* 2007, **129**, 1113.
35 J. H. Gu, C. M. Yam, S. Li, C. Z. Cai, *J. Am. Chem. Soc.,* 2004, **126**, 8098.
36 Z. T. Lin, J. H. Gu, C. H. Li, T. R. Lee, L. X. Xie, S. Chen, P. Y. Cao, S. Jiang, Y. L. Yuan, X. Hong, H. T. Wang, D. Z. Wang, X. F. Wang, G. B. Jiang, M. Heon, T. F. Wu, *Adv. Mater.*, 2017, **29**, 1702090.
37 Zuan‐Tao Lin, Yaxi Li, Jianhua Gu, Huie Wang, Zhuan Zhu, Xia Hong, Zijing Zhang, Qinqin Lu, Jingyi Qiu, Xifan Wang, Jiming Bao, Tianfu Wu, *Adv. Funct. Mater.*, 2018, **28**, 1802482.